Band Structure Calculations of Dispersive Photonic Crystals in 3D using Holomorphic Operator Functions*

Wenqiang Xiao[a], Bo Gong[b,*], Junshan Lin[c], Jiguang Sun[d]

[a]*Beijing Computational Science Research Center, Beijing, 100193, China*
[b]*Faculty of Science, Beijing University of Technology, Beijing, 100124, China*
[c]*Department of Mathematics and Statistics, Auburn University, Auburn, AL 36849, United States*
[d]*Department of Mathematical Sciences, Michigan Technological University, Houghton, MI 49931, United States*

Abstract

We propose a finite element method to compute the band structures of dispersive photonic crystals in 3D. The nonlinear Maxwell's eigenvalue problem is formulated as the eigenvalue problem of a holomorphic operator function. The Nédélec edge elements are employed to discretize the operators, where the divergence free condition for the electric field is realized by a mixed form using a Lagrange multiplier. The convergence of the eigenvalues is proved using the abstract approximation theory for holomorphic operator functions with the regular approximation of the edge elements. The spectral indicator method is then applied to compute the discrete eigenvalues. Numerical examples are presented demonstrating the effectiveness of the proposed method.

Keywords: Band structure, dispersive photonic crystal, Maxwell's equations, nonlinear eigenvalue problem, edge element, holomorphic operator function
2000 MSC: 35P30, 65N25, 65N30, 78M10

*The research of B. Gong is supported partially by China Postdoctoral Science Foundation Grant 2019M650460. The work of J. Lin was supported in part by the NSF grant DMS-2011148. The research of J. Sun is supported partially by the Simons Foundation Grant 711922.

*Corresponding author

Email addresses: `wqxiao@csrc.ac.cn` (Wenqiang Xiao), `gongbo@bjut.edu.cn` (Bo Gong), `jzl0097@auburn.edu` (Junshan Lin), `jiguangs@mtu.edu` (Jiguang Sun)

1. Introduction

Photonic crystals (PCs) are periodic structures with dielectric or metallic materials. They possess band gaps so that the propagation of light through the crystal is prohibited at specific frequencies. This property allows for designs of many optical devices with a wide range of applications, such as filters, optical communications, lasers and microwaves [18]. By the Floquet-Bloch theory [22], the spectral problem related to band structures can be formulated as an eigenvalue problem of the Maxwell's equation with periodic boundary conditions in the fundamental cell.

For non-dispersive media where the permittivity and permeability are independent of the frequency, the eigenvalue problems are linear. Many successful numerical approaches have been proposed, including the plane wave method, the finite-difference time-domain method, the finite element method, the order-N method, the transfer-matrix method, etc [1, 8, 9, 14, 26, 27, 34]. In contrast, dispersive media (with frequency dependent permittivity or permeability) lead to nonlinear eigenvalue problems in general. As such the computation of the band structure is much more challenging. Existing numerical methods for nonlinear eigenvalue problems are mostly based on the Newton's iteration [28], linearization [24] or extensions of the techniques for linear problems [29, 32]. These numerical approaches often require accurate initial guesses of the eigenvalues and eigenvectors, which are not available in general. Furthermore, the convergence analysis of the algorithms is very challenging due to the nonlinearity of the problem. We also refer the readers to [23], which formulates a new stabilized quadratic eigenvalue problem to compute a particular selection of the electromagnetic Bloch variety. The discretization for the 3D Maxwell's equation brings additional difficulty to the eigenvalue computation due to the large degree of freedom (typically in the order of million). Few numerical results exist for the band structure of the dispersive photonic crystals in 3D.

In this paper, we propose a finite element method for band structure calculations of photonic crystals in 3D. Following the idea in [33, 34], we transform the problem into the eigenvalue problem of a holomorphic operator function, whose values are solution operators of the parameterized Maxwell's equations. A mixed formulation for the Maxwell's equations is used to enforce the divergence-free condition and discretized by the Nédélec edge elements. Based on the well-posedness of a related source problem [5], we show that the operator function is of Fredholm type with index zero.

Employing the abstract approximation theory for holomorphic Fredholm operator functions [19, 20] and the finite element theory for Maxwell's equations, we prove the convergence of discrete eigenvalues of the holomorphic operator function. Finally, the spectral indicator method (SIM) is applied to practically calculate the eigenvalues. The SIM extends the ideas in [15, 16] for the generalized eigenvalues of non-Hermitian matrices and is particularly effective for computing eigenvalues of a holomorphic operator function.

The current paper is a non-trivial continuation of [34] in several aspects. First, [34] only deals with the 2D case - a nonlinear eigenvalue problem of the Helmholtz equation, while the current paper deals with the 3D case - a nonlinear eigenvalue problem of the Maxwell's equations. Second, only the TE case is analyzed in [34]. In this paper, a different technique is used and the convergence is proved directly for Maxwell's equations. Third, the 3D numerical examples are way more complicated and there exist only a few examples in literature including the engineering journals. We note that, in the context of finite elements, the above approach has been applied successfully to solve several nonlinear eigenvalue problems of partial differential equations [12, 33].

The current study leads to a convergent finite element approximation for the band structure calculation of 3D dispersive photonic crystals with general frequency-dependent permittivities. This numerical approach is different from the classical finite element theory for linear eigenvalue problems (see, e.g., [2, 4, 30]). The effectiveness of the proposed method is validated by the 3D numerical examples, which are among the very few existing results in literature. The rest of the paper is arranged as follows. In Section 2, we formulate the underlying eigenvalue problem of the Maxwell's systems in mixed form over appropriate functional spaces and write the primal problem as the eigenvalue problem of a holomorphic Fredholm operator function of index zero. Some related theoretical results and the discrete finite element spaces in [5, 11] are recalled in Section 3. The approximation results for the nonlinear operator and the convergence of eigenvalues are proved using the abstract approximation theory of [19, 20]. In Section 4, we write the discrete problem in matrix form and present the SIM-B algorithm to compute the eigenvalues. Finally, numerical examples are presented in Section 5 to illustrate the efficacy of the proposed method. The paper is concluded with some discussions in Section 6.

2. Mathematical Model

We start with the spectral problem for the Maxwell's equations for dispersive photonic crystals in $\mathbb{R}^3$. For simplicity, the medium is assumed to have unit periodicity on a cubic lattice. Let $\mathbb{Z} = \{0, \pm 1, \pm 2, \cdots\}$ and $\Lambda = \mathbb{Z}^3$. We define the periodic domain as the quotient space $D := \mathbb{R}^3/\Lambda$ and let $D_0 = (0,1)^3$ be the reference cell.

Let Ω be a compact set over the complex plane $\mathbb{C}$. For $\omega \in \Omega$, we consider the nonlinear Maxwell's eigenvalue problem

$$\begin{aligned} \nabla \times \left(\frac{1}{\epsilon(x,\omega)} \nabla \times \boldsymbol{H} \right) &= \omega^2 \boldsymbol{H} \quad \text{in } D, \\ \nabla \cdot \boldsymbol{H} &= 0 \qquad\quad \text{in } D, \end{aligned} \tag{1}$$

where $\boldsymbol{H}$ is the magnetic field and $\epsilon(x,\omega)$ is the electric permittivity. $\epsilon(x,\omega)$ depends on the frequency ω and is a periodic function such that

$$\epsilon(x+n,\omega) = \epsilon(x,\omega), \qquad \forall x \in \mathbb{R}^3, n \in \Lambda.$$

We assume that $\epsilon(x,\omega)$ is holomorphic in ω and its real part $\Re\epsilon > 0$. Furthermore, for a fixed $\omega \in \Omega$, $\epsilon_\omega(x) := \epsilon(x,\omega)$ is piecewise constant and uniformly bounded away from zero (see Section 2 of [5]). If there exist some ω and nontrivial $\boldsymbol{H}$ satisfying (1), $(\omega, \boldsymbol{H})$ is called an eigenpair of (1).

Due to the Bloch theory, one seeks for the solutions $(\omega, \boldsymbol{H})$ of (1) such that $\boldsymbol{H}$ is quasi-periodic, i.e.,

$$\boldsymbol{H}(x) = e^{i\boldsymbol{\alpha}\cdot x}\boldsymbol{u}(x) \tag{2}$$

for some periodic function $\boldsymbol{u}$ in x. Let $\boldsymbol{\alpha} = (\alpha_1, \alpha_2, \alpha_3)^T \in \mathbb{R}^3$ be a vector in the first Brillouin zone $\mathcal{K} = [-\pi, \pi]^3$ (see Fig. 1). We introduce the following shifted differential operator:

$$\nabla_{\boldsymbol{\alpha}} = \nabla + i\boldsymbol{\alpha} I,$$

where I is the identity operator. For a given $\boldsymbol{\alpha} \in \mathcal{K}$, it follows from (1) and (2) that

$$\begin{aligned} \nabla_{\boldsymbol{\alpha}} \times \left(\frac{1}{\epsilon(x,\omega)} \nabla_{\boldsymbol{\alpha}} \times \boldsymbol{u} \right) &= \omega^2 \boldsymbol{u} \quad \text{in } D_0, \\ \nabla_{\boldsymbol{\alpha}} \cdot \boldsymbol{u} &= 0 \qquad\quad \text{in } D_0. \end{aligned} \tag{3}$$

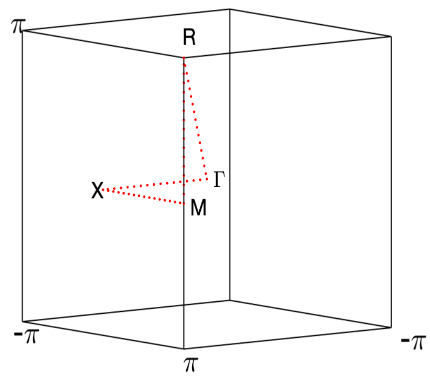

Figure 1: Brillouin zone $\mathcal{K}$.

Now we define several Sobolev spaces of periodic functions. Let $\boldsymbol{L}^2(D_0) = L^2(D_0)^3$ and

$$\begin{aligned}\boldsymbol{H}_p(curl; D_0) &:= \{\boldsymbol{g} \in \boldsymbol{L}^2(D_0) : \nabla \times \boldsymbol{g} \in \boldsymbol{L}^2(D_0) \text{ and } \boldsymbol{g} \text{ periodic in } x\},\\ \boldsymbol{H}_p(div; D_0) &:= \{\boldsymbol{g} \in \boldsymbol{L}^2(D_0) : \nabla \cdot \boldsymbol{g} \in L^2(D_0) \text{ and } \boldsymbol{g} \text{ periodic in } x\},\\ H_p^1(D_0) &:= \{f \in L^2(D_0) : \nabla f \in \boldsymbol{L}^2(D_0) \text{ and } f \text{ periodic in } x\}.\end{aligned}$$

We use following mixed formulation for (3): find $(\omega, \boldsymbol{u}, p) \in \Omega \times \boldsymbol{H}_p(curl; D_0) \times H_p^1(D_0)$ such that

$$\begin{aligned} a(\boldsymbol{u}, \boldsymbol{v}) + b(p, \boldsymbol{v}) &= \omega^2(\boldsymbol{u}, \boldsymbol{v}), \quad \forall \boldsymbol{v} \in \boldsymbol{H}_p(curl; D_0),\\ \overline{b(q, \boldsymbol{u})} &= 0, \qquad\quad \forall q \in H_p^1(D_0),\end{aligned} \tag{4}$$

where

$$a(\boldsymbol{u}, \boldsymbol{v}) = \int_{D_0} \frac{1}{\epsilon(x, \omega)} (\nabla_{\boldsymbol{\alpha}} \times \boldsymbol{u}) \cdot (\overline{\nabla_{\boldsymbol{\alpha}} \times \boldsymbol{v}}) dx, \tag{5}$$

$$b(p, \boldsymbol{v}) = \int_{D_0} \nabla_{\boldsymbol{\alpha}} p \cdot \overline{\boldsymbol{v}} dx, \tag{6}$$

$$(\boldsymbol{u}, \boldsymbol{v}) = \int_{D_0} \boldsymbol{u} \cdot \overline{\boldsymbol{v}} dx. \tag{7}$$

Correspondingly, the source problem associated with (4) for a given $\boldsymbol{f} \in \boldsymbol{L}^2(D_0)$ is to find $(\boldsymbol{u}, p) \in \boldsymbol{H}_p(curl; D_0) \times H_p^1(D_0)$ such that

$$\begin{aligned} a(\boldsymbol{u}, \boldsymbol{v}) + b(p, \boldsymbol{v}) &= (\boldsymbol{f}, \boldsymbol{v}), \quad \forall \boldsymbol{v} \in \boldsymbol{H}_p(curl; D_0), \\ \overline{b(q, \boldsymbol{u})} &= 0, \qquad\quad \forall q \in H_p^1(D_0). \end{aligned} \tag{8}$$

To analyze (8), we introduce the space

$$\mathbb{K} := \{\boldsymbol{v} \in \boldsymbol{H}_p(curl; D_0) : b(q, \boldsymbol{v}) = 0 \ \ \forall q \in H_p^1(D_0)\}.$$

We denote by $\|\cdot\|$ the $\boldsymbol{L}^2(D_0)$ (or $L^2(D_0)$) norm. For a Sobolev space $\mathcal{H}$, we denote its norm by $\|\cdot\|_{\mathcal{H}}$ and its semi-norm by $|\cdot|_{\mathcal{H}}$. Let $C > 0$ be a generic constant. The well-posedness of (8) was analyzed in [5, 11]. The following lemma is from [11] (Theorem 3.1 therein). Note that the case of $\boldsymbol{\alpha} \neq (0,0,0)^T$ with standard boundary conditions was studied in [21].

Lemma 1. *Let $\boldsymbol{\alpha} \in \mathcal{K}$ with $\boldsymbol{\alpha} \neq (0,0,0)^T$. Given $\boldsymbol{u} \in \boldsymbol{L}^2(D_0)$, there exist unique functions $\boldsymbol{w} \in (H_p^1(D_0))^3$ and $\phi \in H_p^1(D_0)$ satisfying*

$$\begin{aligned} \boldsymbol{u} =& \nabla_{\boldsymbol{\alpha}} \times \boldsymbol{w} + \nabla_{\boldsymbol{\alpha}} \phi \quad \text{with} \quad \nabla_{\boldsymbol{\alpha}} \cdot \boldsymbol{w} = 0, \\ \|\boldsymbol{w}\|_1 &+ \|\phi\|_1 \leq C\|\boldsymbol{u}\|. \end{aligned}$$

Let $\boldsymbol{u}$ and p be the solutions of (8). Then it can be shown that

$$\|\boldsymbol{u}\|_1 + \|p\|_1 \leq C\|\boldsymbol{f}\|. \tag{9}$$

Furthermore, for a fixed $\omega \in \Omega$, there exists a linear operator T_ω such that, for $\boldsymbol{f} \in \boldsymbol{L}^2(D_0)$,

$$T_\omega \boldsymbol{f} = \boldsymbol{u},$$

where $\boldsymbol{u}$ is the first component of the solution of (8). The readers are referred to [5, 11] for the detailed proof. Note that T_ω is a compact operator since the embedding of $\boldsymbol{H}_p(curl; D_0) \cap \boldsymbol{H}_p(div; D_0) \subset H_p^1(D_0)^3$ is compact (Lemma 2 in [5]). Consequently, we obtain an operator function $T(\omega) : \Omega \to \mathcal{L}(\boldsymbol{L}^2(D_0), \boldsymbol{L}^2(D_0))$ such that $T(\omega) := T_\omega$.

From the above discussions, we see that (4) is equivalent to the eigenvalue problem of the operator function T:

$$T(\omega)(\omega^2 \boldsymbol{u}) = \boldsymbol{u} \quad \omega \in \Omega.$$

Define a nonlinear operator function $F : \Omega \to \mathcal{L}(\boldsymbol{L}^2(D_0), \boldsymbol{L}^2(D_0))$ by

$$F(\omega) = T(\omega) - \frac{1}{\omega^2} I \quad \omega \in \Omega. \tag{10}$$

It is clear that ω is an eigenvalue of (4) if and only if ω is an eigenvalue of the operator function F, i.e., there exists $\boldsymbol{u}$ such that $F(\omega)\boldsymbol{u} = 0$. The following lemma shows that F is a holomorphic operator function.

Lemma 2. *The operator function $T : \Omega \to \mathcal{L}(\boldsymbol{L}^2(D_0), \boldsymbol{L}^2(D_0))$ is holomorphic.*

Proof. For simplicity, we omit the x and write $\epsilon(\omega)$ for $\epsilon(x, \omega)$. Let $\omega \in \Omega$ and $\delta\omega$ be small enough such that $\omega + \delta\omega \in \Omega$. Since $\epsilon(\omega)$ is holomorphic in Ω, one has that

$$\epsilon(\omega + \delta\omega) - \epsilon(\omega) = \epsilon'(\omega)(\delta\omega) + o(|\delta\omega|). \tag{11}$$

For a $\boldsymbol{f} \in \boldsymbol{L}^2(D_0)$, let $\boldsymbol{u} := T(\omega)\boldsymbol{f}$, i.e., $\boldsymbol{u} \in \mathbb{K}$ is such that

$$\int_{D_0} \frac{1}{\epsilon(\omega)} \nabla_{\boldsymbol{\alpha}} \times \boldsymbol{u} \cdot \overline{\nabla_{\boldsymbol{\alpha}} \times \boldsymbol{v}} dx = (\boldsymbol{f}, \boldsymbol{v}), \quad \forall \boldsymbol{v} \in \mathbb{K}$$

Let $\boldsymbol{w} := T(\omega + \delta\omega)\boldsymbol{f}$, i.e., $\boldsymbol{w} \in \mathbb{K}$ is such that

$$\int_{D_0} \frac{1}{\epsilon(\omega + \delta\omega)} \nabla_{\boldsymbol{\alpha}} \times \boldsymbol{w} \cdot \overline{\nabla_{\boldsymbol{\alpha}} \times \boldsymbol{v}} dx = (\boldsymbol{f}, \boldsymbol{v}) \quad \forall \boldsymbol{v} \in \mathbb{K}.$$

Then

$$\int_{D_0} \left(\frac{1}{\epsilon(\omega)} \nabla_{\boldsymbol{\alpha}} \times \boldsymbol{u} - \frac{1}{\epsilon(\omega + \delta\omega)} \nabla_{\boldsymbol{\alpha}} \times \boldsymbol{w} \right) \cdot \overline{\nabla_{\boldsymbol{\alpha}} \times \boldsymbol{v}} dx = 0.$$

Due to (11), we have that, for all $\boldsymbol{v} \in \mathbb{K}$,

$$\begin{aligned} &\int_{D_0} \frac{1}{\epsilon(\omega)} \nabla_{\boldsymbol{\alpha}} \times (\boldsymbol{u} - \boldsymbol{w}) \cdot \overline{\nabla_{\boldsymbol{\alpha}} \times \boldsymbol{v}} dx \\ = &-\int_{D_0} \frac{\epsilon(\omega + \delta\omega) - \epsilon(\omega)}{\epsilon(\omega)\epsilon(\omega + \delta\omega)} \nabla_{\boldsymbol{\alpha}} \times \boldsymbol{w} \cdot \overline{\nabla_{\boldsymbol{\alpha}} \times \boldsymbol{v}} dx \\ = &-\int_{D_0} \frac{\epsilon'(\omega)(\delta\omega) + o(|\delta\omega|)}{\epsilon(\omega)\epsilon(\omega + \delta\omega)} \nabla_{\boldsymbol{\alpha}} \times \boldsymbol{w} \cdot \overline{\nabla_{\boldsymbol{\alpha}} \times \boldsymbol{v}} dx. \end{aligned}$$

Thus $T(\omega)$ is continuous in Ω. Let $\boldsymbol{\phi} \in \mathbb{K}$ be the solution of

$$\int_{D_0} \frac{1}{\epsilon(\omega)} \nabla_{\boldsymbol{\alpha}} \times \boldsymbol{\phi} \cdot \overline{\nabla_{\boldsymbol{\alpha}} \times \boldsymbol{v}} dx = - \int_{D_0} \frac{\epsilon'(\omega)}{\epsilon^2(\omega)} \nabla_{\boldsymbol{\alpha}} \times \boldsymbol{u} \cdot \overline{\nabla_{\boldsymbol{\alpha}} \times \boldsymbol{v}} dx \quad \forall \boldsymbol{v} \in \mathbb{K} \tag{12}$$

Since $\epsilon(\omega)$ is bounded, straightforward calculations show that

$$\left\| \frac{\boldsymbol{u} - \boldsymbol{w}}{\delta\omega} - \boldsymbol{\phi} \right\| \to 0 \quad \text{as} \quad \delta\omega \to 0.$$

Hence $T(\omega)\boldsymbol{f}$ is holomorphic on Ω. By Theorem 1.7.1 of [13], $T(\omega)$ is holomorphic .

□

By virtue of (10), F is a holomorphic Fredholm operator function of index zero on Ω if $\Omega \subset \mathbb{C} \setminus \{0\}$ is compact [13, 19].

3. FEM Discretization and Convergence

In this section, using the modified edge elements for (8), we propose a discretization F_h for F and prove the convergence of the operator F_h as $h \to 0$. Then we show that the eigenvalues of F_h converges to those of F employing the abstract convergence theory.

Let $\mathcal{T}_h$ be a tetrahedra mesh for D_0 with mesh size h. We shall use the modified approximation spaces for $H^1_p(D_0)$, $\boldsymbol{H}_p(curl; D_0)$, $\boldsymbol{H}_p(div; D_0)$, $L^2(D_0)$ with respect to $\mathcal{T}_h$, which are generated by multiplying $\boldsymbol{\alpha}$-phase function with usual basis functions [5, 10, 11]. For simplicity, we employ the lowest order edge element of the first family and linear Lagrange element to discretize (8) [25, 7]. The results can be extended to higher order or second family edge elements.

Let $\widetilde{\boldsymbol{V}}_h \subset \boldsymbol{H}_p(curl; D_0)$ be the edge element space and $\widetilde{W}_h \subset H^1_p(D_0)$ be the Lagrange element space. The basis functions for $\widetilde{\boldsymbol{V}}_h$ and $\widetilde{W}_h$ are denoted by $\{\widetilde{\Psi}_j\}_{j=1,\cdots,N_1}$ and $\{\widetilde{\phi}_j\}_{j=1,\cdots,N_2}$, respectively. We define the $\boldsymbol{\alpha}$-modified finite element spaces:

$$\boldsymbol{V}^{\alpha}_h = \text{span}\{e^{-i\boldsymbol{\alpha}\cdot(x-x_j)}\widetilde{\Psi}_j\}_{j=1,\cdots,N_1},$$
$$W^{\alpha}_h = \text{span}\{e^{-i\boldsymbol{\alpha}\cdot(x-y_j)}\widetilde{\phi}_j\}_{j=1,\cdots,N_2}.$$

Here x_j is the center of the jth edge and y_j is the vertex corresponding to the nodal basis function $\widetilde{\phi}_j$. The degrees of freedom for the spaces W^{α}_h are again the nodal values. The space $\boldsymbol{V}_h^\alpha$ inherits the degrees of freedom from $\widetilde{\boldsymbol{V}}_h$, i.e.,

$$v_j^\alpha(\Psi) = \frac{1}{|e_j|}\int_{e_j} e^{i\boldsymbol{\alpha}\cdot(x-x_j)}\Psi\cdot\boldsymbol{\tau}_j ds, \quad \Psi\in\boldsymbol{V}_h^\alpha,$$

where e_j is an edge and $\boldsymbol{\tau}_j$ is the unit tangent vector along e_j. Given a sufficiently smooth vector function $\boldsymbol{g}$, we define the interpolation operator

$$\pi_h^\alpha \boldsymbol{g} = \sum_j v_j^\alpha(\boldsymbol{g}) e^{-i\boldsymbol{\alpha}\cdot(x-x_j)}\widetilde{\Psi}_j.$$

The spaces $\boldsymbol{V}_h^\alpha$ and W_h^α are the modified approximation spaces for $\boldsymbol{H}_p(curl; D_0)$ and $H_p^1(D_0)$, respectively. The modified approximation spaces for $\boldsymbol{H}_p(div; D_0)$ and $L^2(D_0)$ can be defined analogously [10, 11, 5]. They satisfy the commuting diagram property with respect to the differential operators $\nabla_{\boldsymbol{\alpha}}, \nabla_{\boldsymbol{\alpha}}\times, \nabla_{\boldsymbol{\alpha}}\cdot$ (see Theorem 4.1 of [11]).

The discrete problem for (8) is to find $(\boldsymbol{u}_h, p_h)\in\boldsymbol{V}_h^\alpha\times W_h^\alpha$ such that

$$\begin{aligned} a(\boldsymbol{u}_h,\boldsymbol{v}_h) + b(p_h,\boldsymbol{v}_h) &= (\boldsymbol{f},\boldsymbol{v}_h), \quad \forall \boldsymbol{v}_h\in\boldsymbol{V}_h^\alpha, \\ \overline{b(q_h,\boldsymbol{u}_h)} &= 0, \qquad\quad \forall q_h\in W_h^\alpha. \end{aligned} \tag{13}$$

The corresponding discrete space of $\mathbb{K}$ is

$$\mathbb{K}_h = \{\boldsymbol{u}_h\in\boldsymbol{V}_h^\alpha : b(q_h,\boldsymbol{u}_h) = 0, \quad \forall q_h\in W_h^\alpha\}.$$

The well-posedness of the discrete problem (13) can be established by verifying the discrete coercivity of $a(\boldsymbol{v}_h,\boldsymbol{v}_h)$ on $\mathbb{K}_h$ and the discrete inf-sup condition $b(q_h,\boldsymbol{v}_h)$ on $W_h^\alpha\times\boldsymbol{V}_h^\alpha$.

Following [5, 11], we assume that the solution $\boldsymbol{u}$ of (8) satisfies

$$\begin{aligned} \boldsymbol{u} &\in H^s(D_0)^3, &&\text{for some } s > \frac{1}{2}, \\ \nabla\times\boldsymbol{u} &\in H^r(D_0)^3, &&\text{for some } r > 0. \end{aligned} \tag{14}$$

We have the following convergence result.

Lemma 3. *Let* $(\boldsymbol{u}, p)\in\boldsymbol{H}_p(curl; D_0)\times H_p^1(D_0)$ *be solution of* (8)*, and* $(\boldsymbol{u}_h, p_h)\in\boldsymbol{V}_h^\alpha\times W_h^\alpha$ *be solution of* (13)*. Assume that* $\boldsymbol{u}$ *satisfies the regularity assumption* (14) *and* $p\in H^2(D_0)$*. Then*

$$\|\boldsymbol{u}-\boldsymbol{u}_h\| \le Ch^t(|\boldsymbol{u}|_s + \|\nabla\times\boldsymbol{u}\|_r), \quad \text{where } t = \min\{s, r\}. \tag{15}$$

Proof. Under the conditions of lemma, there is an element $\boldsymbol{u}^I \in \mathbb{K}_h$ satisfying (see Lemma 9 of [5])

$$\|\boldsymbol{u} - \boldsymbol{u}^I\|_{curl} \leq Ch^t(|\boldsymbol{u}|_s + \|\nabla \times \boldsymbol{u}\|_r). \tag{16}$$

For the mixed formulations (8) and (13), we have the following error estimations [6, Theorem 5.2.5],

$$\|\boldsymbol{u} - \boldsymbol{u}_h\|_{curl} \leq C \left(\inf_{\boldsymbol{v}_h \in K_h} \|\boldsymbol{u} - \boldsymbol{v}_h\|_{curl} + \inf_{q_h \in W_h^\alpha} \|p - q_h\|_1 \right).$$

By (16) and the standard interpolation error bounds for Lagrange elements [7], we have

$$\|\boldsymbol{u} - \boldsymbol{u}_h\|_{curl} \leq C \left(h^t(|\boldsymbol{u}|_s + \|\nabla \times \boldsymbol{u}\|_r) + h\|p\|_2 \right) \leq Ch^t.$$

Hence,

$$\|\boldsymbol{u} - \boldsymbol{u}_h\| \leq \|\boldsymbol{u} - \boldsymbol{u}_h\|_{curl} \leq Ch^t.$$

□

Using the convergence of the mixed finite element method (13) for the source problem (8), we are now ready to define the discrete operator function $F_h(\omega)$ and prove the convergence of the eigenvalues of $F_h(\omega)$ to those of $F(\omega)$.

Define the L^2-projection $\mathcal{P}_h : \boldsymbol{L}^2(D_0) \to \boldsymbol{V}_h^\alpha$ such that

$$(\boldsymbol{f}, \boldsymbol{v}_h) = (\mathcal{P}_h \boldsymbol{f}, \boldsymbol{v}_h), \quad \forall \boldsymbol{v}_h \in \boldsymbol{V}_h^\alpha. \tag{17}$$

For a fixed $\omega \in \Omega$, let $\boldsymbol{u}_h$ be the solution of (13). The well-posedness of (13) implies $\|\boldsymbol{u}_h\| \leq \|\mathcal{P}_h \boldsymbol{f}\|$. The discrete solution operator $T_h(\omega)$ for (13) is such that $T_h(\omega)\mathcal{P}_h \boldsymbol{f} = \boldsymbol{u}_h$. Now we define the discrete operator function $F_h : \Omega \to \mathcal{L}(\boldsymbol{V}_h^\alpha, \boldsymbol{V}_h^\alpha)$ as

$$F_h(\omega) = T_h(\omega) - \frac{1}{\omega^2} I, \quad \omega \in \Omega. \tag{18}$$

For simplicity, in the rest of paper, we denote $\mathcal{P}_h \boldsymbol{f}$ by $\boldsymbol{f}_h$ and $\boldsymbol{V}_h$ by $\boldsymbol{V}_h^\alpha$.

The error estimate (15) and the well-posedness of (8) imply that

$$\|\boldsymbol{u} - \boldsymbol{u}_h\| \leq Ch^t(|\boldsymbol{u}|_s + \|\nabla \times \boldsymbol{u}\|_r) \leq Ch^t\|\boldsymbol{f}\|. \tag{19}$$

Consequently,

$$\|T(\omega) - T_h(\omega)\mathcal{P}_h\| \leq Ch^t.$$

Due to the fact that

$$\|F(\omega)\boldsymbol{v}_h - F_h(\omega)\boldsymbol{v}_h\| = \|T(\omega)\boldsymbol{v}_h - T_h(\omega)\boldsymbol{v}_h\| \le \|T(\omega) - T_h(\omega)\mathcal{P}_h\|\|\boldsymbol{v}_h\|, \ \forall \boldsymbol{v}_h \in \boldsymbol{V}_h,$$

we obtain that

$$\|F(\omega)|_{\boldsymbol{V}_h} - F_h(\omega)\| \le Ch^t. \tag{20}$$

The following lemma is obvious for the L^2-projection $\mathcal{P}_h$.

Lemma 4. *For all $\boldsymbol{f} \in \boldsymbol{L}^2(D_0)$, $\|\boldsymbol{f} - \mathcal{P}_h\boldsymbol{f}\| \to 0$ as $h \to 0$.*

Lemma 5. *Assume that $\Omega \subset \mathbb{C}\backslash\{0\}$ is compact. There exists $h_0 > 0$ small enough such that*

$$\sup_{h<h_0}\sup_{\omega\in\Omega}\|F_h(\omega)\| < \infty. \tag{21}$$

Proof. Assume $\boldsymbol{f}_h \in \boldsymbol{V}_h$. Then

$$\|F_h(\omega)\boldsymbol{f}_h\| = \|T_h(\omega)\boldsymbol{f}_h - \frac{1}{\omega^2}\boldsymbol{f}_h\| \le \|\boldsymbol{u}_h\| + \frac{1}{\omega^2}\|\boldsymbol{f}_h\| \le C\|\boldsymbol{f}_h\|.$$

The last inequality is due to the well-posedness of the discrete problem (13) and the fact that $\Omega \subset \mathbb{C}\backslash\{0\}$ is compact. □

Lemma 6. *Assume $\boldsymbol{f} \in \boldsymbol{L}^2(D_0)$, then $\lim_{h\to 0}\|F_h(\omega)\mathcal{P}_h\boldsymbol{f} - \mathcal{P}_hF(\omega)\boldsymbol{f}\| = 0$.*

Proof. Using the definitions of F and F_h and Lemmas 4 and 3, we obtain that

$$\begin{aligned}\|F_h(\omega)\mathcal{P}_h\boldsymbol{f} - \mathcal{P}_hF(\omega)\boldsymbol{f}\| &= \left\|T_h(\omega)\mathcal{P}_h\boldsymbol{f} - \frac{1}{\omega^2}\mathcal{P}_h\boldsymbol{f} - \mathcal{P}_hT(\omega)\boldsymbol{f} + \mathcal{P}_h(\frac{1}{\omega^2}\boldsymbol{f})\right\| \\ &= \|T_h(\omega)\mathcal{P}_h\boldsymbol{f} - \mathcal{P}_hT(\omega)\boldsymbol{f}\| \\ &= \|\boldsymbol{u}_h - \boldsymbol{u} + \boldsymbol{u} - \mathcal{P}_h\boldsymbol{u}\| \\ &\le \|\boldsymbol{u} - \boldsymbol{u}_h\| + \|\boldsymbol{u} - \mathcal{P}_h\boldsymbol{u}\| \\ &\le Ch^t. \end{aligned} \tag{22}$$

The proof is complete by taking $h \to 0$. □

Now we are ready to present the convergence theorem for the eigenvalues of F_h. Its proof is to verify the conditions (b1)-(b4) and then employ Theorem 2 in Appendix.

Theorem 1. *Let $\omega_0 \in \sigma(F)$. Assume that h is small enough. Then there exists $\{\omega_h \in \sigma(F_h)\}$ such that $\omega_h \to \omega_0$ as $h \to 0$ and the following estimate holds*

$$|\omega_h - \omega_0| \leq Ch^{\frac{t}{\kappa}}, \tag{23}$$

where κ is the maximum rank of the eigenvectors associated with ω_0 (see Definition 4 in Appendix).

Proof. Let $\{h_n\}$ be a sequence of sufficiently small positive numbers with $h_n \to 0$ as $n \to \infty$ and $F_n(\omega) := F_{h_n}(\omega)$, $\boldsymbol{V}_n := \boldsymbol{V}_{h_n}$ and $p_n := \mathcal{P}_{h_n}$.

Due to Lemma 4, (b1) holds with $X = Y = \boldsymbol{L}^2(D_0)$, $X_n = Y_n = \boldsymbol{V}_n$, and $q_n = p_n$. (b2) and (b3) hold due to Lemma 5 and Lemma 6.

Next we verify (b4). Assume that $\boldsymbol{v}_n \in \boldsymbol{V}_n$, $n \in \mathbb{N}' \subset \mathbb{N}$ with $\|\boldsymbol{v}_n\| \leq 1$ and

$$\lim_{n\to\infty} \|F_n(\omega)\boldsymbol{v}_n - p_n\boldsymbol{y}\| = 0, \tag{24}$$

for some $\boldsymbol{y} \in \boldsymbol{L}^2(D_0)$. Let $\rho(F)$ and $\sigma(F)$ be resolvent set $\rho(F)$ and the spectrum of F, respectively (see (A.2)). In the following, we consider $\omega \in \rho(F)$ and $\omega \in \sigma(F)$ separately.

Let $\omega \in \rho(F)$. Then $F(\omega)^{-1}$ exists and is bounded. Let $\boldsymbol{v} = F(\omega)^{-1}\boldsymbol{y}$. We have

$$\begin{aligned}\boldsymbol{v}_n - p_n\boldsymbol{v} = F(\omega)^{-1}\big(&(F(\omega) - F_n(\omega))(\boldsymbol{v}_n - p_n\boldsymbol{v}) \\ &+ F_n(\omega)\boldsymbol{v}_n - p_nF(\omega)\boldsymbol{v} + p_nF(\omega)\boldsymbol{v} - F_n(\omega)p_n\boldsymbol{v}\big).\end{aligned}$$

Recalling that $\|F(\omega)|_{\boldsymbol{V}_n} - F_n(\omega)\| \leqslant Ch_n^t$ from (20), it holds that

$$\begin{aligned}\|\boldsymbol{v}_n - p_n\boldsymbol{v}\| \leqslant C\big(&h_n^t\|\boldsymbol{v}_n - p_n\boldsymbol{v}\| \\ &+ \|F_n(\omega)\boldsymbol{v}_n - p_nF(\omega)\boldsymbol{v}\| + \|p_nF(\omega)\boldsymbol{v} - F_n(\omega)p_n\boldsymbol{v}\|\big).\end{aligned} \tag{25}$$

Using (24) and Lemma 6 we have that

$$\|\boldsymbol{v}_n - p_n\boldsymbol{v}\| \to 0 \quad \text{as } n \to \infty.$$

Let $\omega \in \sigma(F)$. Denote by $E(\omega)$ the finite dimensional eigenspace of ω [19] and by $P_{E(\omega)}$ the projection from $\boldsymbol{L}^2(D)$ to $E(\omega)$. Let $F(\omega)^{-1}$ be the inverse of $F(\omega)|_{\boldsymbol{L}^2(D)/E(\omega)}$ from $\mathcal{R}(F(\omega))$ to $\boldsymbol{L}^2(D)/E(\omega)$. Due to (24), we have that

$$\|F(\omega)\boldsymbol{v}_n - \boldsymbol{y}\| \leqslant \|F(\omega)\boldsymbol{v}_n - F_n(\omega)\boldsymbol{v}_n\| + \|F_n(\omega)\boldsymbol{v}_n - p_n\boldsymbol{y}\| + \|p_n\boldsymbol{y} - \boldsymbol{y}\| \to 0,$$

as $n \to \infty$. Since $\mathcal{R}(F(\omega))$ is closed, $\boldsymbol{y} \in \mathcal{R}(F(\omega))$.

Let $\boldsymbol{v}' := F(\omega)^{-1}\boldsymbol{y}$ and $\boldsymbol{v}'_n := (I - p_n P_{E(\omega)})\boldsymbol{v}_n$. Similar to (25), we deduce that

$$\begin{aligned}&\|\boldsymbol{v}'_n - p_n\boldsymbol{v}'\|\\ &\leqslant (1 - Ch_n^t)^{-1}C\big(\|F_n(\omega)\boldsymbol{v}'_n - p_nF(\omega)\boldsymbol{v}'\| + \|p_nF(\omega)\boldsymbol{v}' - F_n(\omega)p_n\boldsymbol{v}'\|\big) \to 0.\end{aligned}$$

On the other hand, since $E(\omega)$ is finite dimensional, there is a subsequence $\mathbb{N}''$ and $\boldsymbol{v}'' \in E(\omega)$ such that $\|P_{E(\omega)}\boldsymbol{v}_n - \boldsymbol{v}''\| \to 0$ as $\mathbb{N}'' \ni n \to \infty$. Therefore we have that

$$\|\boldsymbol{v}_n - p_n\boldsymbol{v}\| \leqslant \|\boldsymbol{v}'_n - p_n\boldsymbol{v}'\| + \|p_nP_{E(\omega)}\boldsymbol{v}_n - p_n\boldsymbol{v}''\| \to 0, \quad \text{as} \quad \mathbb{N}'' \ni n \to \infty,$$

where $\boldsymbol{v} := \boldsymbol{v}' + \boldsymbol{v}''$. We have verified (b1)-(b4) and (23) follows Theorem 2. The proof is complete. □

Corollary 1. *If ω_0 is a simple eigenvalue, i.e., $\kappa = 1$, one has that*

$$|\omega - \omega_h| \leq Ch^t. \tag{26}$$

4. Spectrum Indicator Method

The discrete form of (4) is to find $\omega \in \Omega$ and $(\boldsymbol{u}_h, p_h) \in \boldsymbol{V}_h^\alpha \times W_h^\alpha$ such that

$$\begin{aligned} a(\boldsymbol{u}_h, \boldsymbol{v}_h) + b(p_h, \boldsymbol{v}_h) &= \omega^2(\boldsymbol{u}_h, \boldsymbol{v}_h), \quad \forall \boldsymbol{v}_h \in \boldsymbol{V}_h^\alpha,\\ \overline{b(q_h, \boldsymbol{u}_h)} &= 0, \qquad \forall q_h \in W_h^\alpha. \end{aligned} \tag{27}$$

Given $\boldsymbol{\alpha} \in \mathcal{K}$, (27) can be written as the following matrix eigenvalue problem

$$\begin{bmatrix} A(\omega) & B^H \\ B & 0 \end{bmatrix} \begin{bmatrix} u \\ p \end{bmatrix} = \omega^2 \begin{bmatrix} M & 0 \\ 0 & 0 \end{bmatrix} \begin{bmatrix} u \\ p \end{bmatrix}, \tag{28}$$

where $A(\omega)$ is the matrix associated to the sesquilinear form $a(\cdot,\cdot)$ defined in (5), B is the matrix associated to $b(\cdot,\cdot)$ defined in (6) and M is the mass matrix. Consequently, the eigenvalues of $F_h(\omega)$ are the eigenvalues of $\mathbb{F}_h(\omega)$ given by

$$\mathbb{F}_h(\omega) := \begin{bmatrix} A(\omega) & B^H \\ B & 0 \end{bmatrix} - \omega^2 \begin{bmatrix} M & 0 \\ 0 & 0 \end{bmatrix}. \tag{29}$$

To compute the eigenvalues of $\mathbb{F}_h$, which are complex in general, we design a new version of the spectral indicator method (SIM) proposed in [15, 16, 17]. Without loss of generality, let $\Omega \subset \mathbb{C}$ be a square and Θ be the circle circumscribing Ω. Assume that $\Theta \subset \rho(\mathbb{F}_h)$ such that $\mathbb{F}_h(\omega)^{-1}$ exists and is bounded for $\omega \in \Theta$. Define an operator

$$\mathcal{G} = \frac{1}{2\pi i} \int_{\Theta} \mathbb{F}_h(\omega)^{-1} d\omega, \tag{30}$$

where $i = \sqrt{-1}$. Let g_h be a random vector. If $\mathbb{F}_h$ has no eigenvalues inside Θ, then $\mathcal{G}g_h = 0$. If $\mathbb{F}_h$ has at least one eigenvalue inside Θ, then $\mathcal{G}g_h \neq 0$ almost surely. Thus $|\mathcal{G}g_h|$ can be used as an indicator for the location of eigenvalues. If Θ contains eigenvalues inside, Ω is subdivided into smaller squares, and the procedure continues until the eigenvalues are identified in a small enough square.

In practice, one does not invert $\mathbb{F}_h(\omega)$ but solves $f_h(\omega)$ for $\mathbb{F}_h(\omega) f_h = g_h$. Using the trapezoidal rule for the integral (30), we define an indicator I_Ω for Ω as

$$I_\Omega := \frac{1}{L} \left| \sum_{j=1}^{n_0} \mathrm{w}_j f_h(\omega_j) \right|, \tag{31}$$

where L is the length of Θ, ω_j's and w_j's are the quadrature points and weights, respectively. The indicator I_Ω is used to decide if Ω contains eigenvalues or not. If $I_\Omega > \delta_0$ for some threshold $\delta_0 > 0$, there exists at least one eigenvalue in Ω. In such a case, Ω is called admissible and uniformly divided into smaller squares. The indicators of these small squares are computed and the admissible squares are subdivided. The procedure continues until the size of the squares is smaller than a specified precision ϵ_0, e.g., $\epsilon_0 = 10^{-6}$. The centers of the squares are the approximated eigenvalues

The following algorithm SIM-B computes all the eigenvalues of $\mathbb{F}_h$ in Ω.

SIM-B:

- Given a series of congruent squares $\{\Omega_n^0\}_{n=1}^{N_0}$ covering Ω.
- Choose the precision ϵ_0 and the indicator threshold δ_0.

1. Generate a tetrahedral mesh for D_0.
2. Let f_h be a normalized random vector and set level $i = 0$.
3. At level i, if the size of the squares at level i is larger than ϵ_0, do

- For each square $\Omega_n^i, n = 1, \ldots, N_i$ at the current level, evaluate $I_{\Omega_n^i}$ using (31).
- If $|I_{\Omega_n^i}| > \delta_0$, uniformly divide Ω_n^i into small squares and leave them to the next level.
- $i + 1 \rightarrow i$.

4. Output eigenvalues.

The reason for taking Ω to be a square is that a compact region can be covered by squares and it is easily to divide a square into smaller squares. The use of Θ is due to the exponential convergence of the trapezoidal rule. There are some gaps between Θ and Ω. But they are smaller than the specified precision at the end of the procedure and can be ignored. We refer the readers to [12, 15, 16, 33, 34] for more discussions and applications of SIMs.

5. Numerical Examples

In the section, we present several numerical examples and show the dispersion relations $\omega(\boldsymbol{\alpha})$ with $\boldsymbol{\alpha}$ moving along $\Gamma \rightarrow X \rightarrow M \rightarrow R$ in the Brillouin zone (Fig. 1). The fundamental cell is the unit cube $D_0 = [0, 1]^3$. The photonic crystal consists of two components, the air and a dielectric material, i.e., $\epsilon = \epsilon_b$ in $D_1 \subset D_0$ and $\epsilon = \epsilon_a = 1$ in $D_0 \setminus D_1$. The lowest order edge element of the first family and the linear Lagrange element are used on a tetrahedral mesh of D_0. All calculations were performed on a tetrahedral mesh with $h \approx 1/16$. We take $\Omega = [0.2, 6.2] \times [-3, 3], N_0 = 1, n_0 = 16$ in our examples.

Example 1. For validation of the proposed method, we first consider a non-dispersive electric permittivity such that (1) becomes a linear eigenvalue problem. The holomorphic operator function is simply $F_h(\omega) = T_h - \frac{1}{\omega^2} I$. The structure consists of a silicon frame (D_1) embedded in air shown in Fig. 2 (left). The colored part represents silicon and the blank part represents air. The frame thickness is 0.125 in the unit cube with $\epsilon_b = 13$ for silicon. This model is called the scaffold structure. The dispersion diagram is shown in Fig. 2 (right), in which a spectral gap appears in the band structure. The numerical result is consistent with Fig. 2 of [10]. Note that in order to compare with the Fig. 2 of [10], we set the value of y-axis to $\omega/(2\pi)$ in Fig. 2.

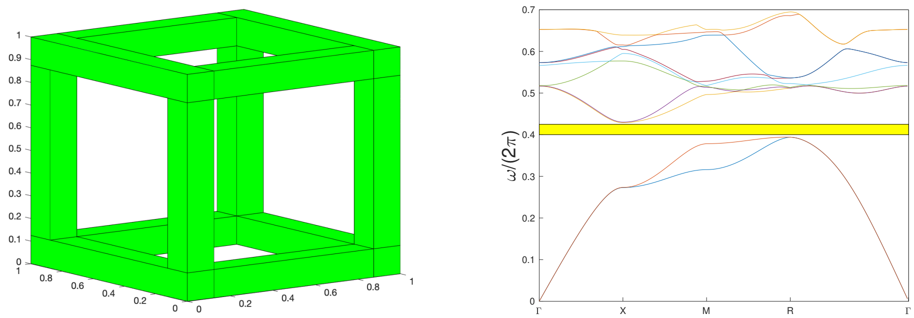

Figure 2: Example 1. Left: Scaffold structure in unit cell. Right: The dispersion diagram with a band gap (the yellow part).

Example 2. We consider a dispersive photonic crystal in this example. The frequency-dependent electric permittivity function is given by

$$\epsilon_b(\omega) = \epsilon_\infty \frac{\omega_L^2 - \omega^2}{\omega_T^2 - (1+\gamma i)\omega^2}, \tag{32}$$

where ϵ_∞ is the optical frequency dielectric constant, ω_L and ω_T are the frequencies of the longitudinal optical and transverse optical vibration modes of infinite wavelength, respectively, γ is a constant. In the computation, $\epsilon_\infty = 20, \omega_T = 8.12$THz, $\omega_L = 8.75$THz, $\gamma = 0.02$. Note that the eigenvalues are complex with small imaginary parts. We use the real parts of the eigenvalues for the dispersion diagrams shown in Fig. 3. It is seen that the photonic structure attains a spectral gap between two bands.

Example 3. The structure of the photonic crystal is shown Fig. 4 (left). The frequency-dependent electric permittivity is

$$\epsilon_b(\omega) = 5.8 + \epsilon_\infty \frac{\omega_L^2 - 1.2\omega^2 - 2\omega^3 + 3.64\omega^4}{\omega_T^2 - 2.6\omega - 1.2\omega^2 - \omega^3}, \tag{33}$$

We set $\epsilon_\infty = 18.6$, $\omega_T = 9.89$THz, $\omega_L = 10.45$THz. The computational band structure is demonstrated in Fig. 4 (right), where a band gap is also obtained.

6. Conclusions

We propose a novel numerical method for the band structure calculations of 3D dispersive photonic crystals. The nonlinear Maxwell's eigenvalue problem is first reformulated as the eigenvalue problem of a holomorphic operator

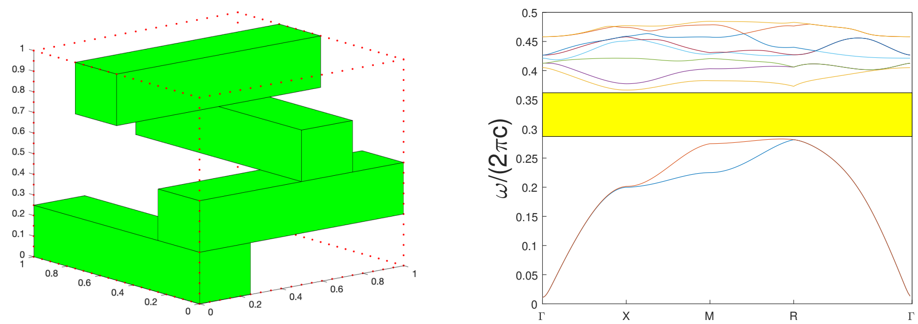

Figure 3: Example 2. Left: Unit cell. Right: The dispersion diagram with a band gap (the yellow part), c is the speed of light.

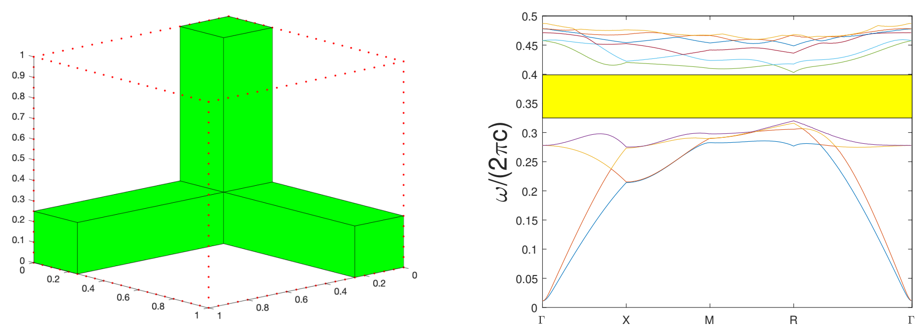

Figure 4: Example 3. Left: The structure of the photonic crystal. Right: The dispersion diagram with a band gap (the yellow part), c is the speed of light.

function. Using the well-posedness results of the related source problem, we show that the operator function is Fredholm. A mixed finite element method is then employed to discretize the operator. The convergence of the eigenvalues are proved by combining the convergence of the finite element method for the source problem and the abstract approximation theory for holomorphic Fredholm operator functions. Finally the spectrum indicator method is applied to practically compute eigenvalues, which require no a priori information on the spectral distribution. The effectiveness of the proposed approach is demonstrated by several numerical examples in 3D, which are among the very few in literature.

Efficient computation of 3D band structures is challenging due to the large number of degrees of freedom of the discrete system. The evaluation of the indicators (31) needs to solve many linear systems. Fortunately, the SIM is highly scalable. Currently, combining with domain decompositions, we are working on a parallel version of SIM to treat 3D photonic crystals on finer meshes.

Appendix A. Holomorphic Fredholm Operator Function and Its Abstract Approximation Theory

We present some preliminaries on holomorphic Fredholm operator functions and the abstract approximation theory of the associated eigenvalue problems [13, 19, 20, 3]. Let X, Y be complex Banach spaces and we denote by $\mathcal{L}(X, Y)$ as the space of bounded linear operators from X to Y. $\Omega \subset \mathbb{C}$ is a compact and simply connected set.

Definition 1. *Let $\mathcal{B}$ be a Banach space and $\Omega \subset \mathbb{C}$ be an open set. A function $f : \Omega \to \mathcal{B}$ is called holomorphic if, for each $w \in \Omega$,*

$$f'(w) := \lim_{z \to w} \frac{f(z) - f(w)}{z - w}$$

exists.

Definition 2. *An operator $A \in \mathcal{L}(X, Y)$ is said to be Fredholm if*

1. *the range of A, denoted by $\mathcal{R}(A)$, is closed in Y;*
2. *the null space of A, denoted by $\mathcal{N}(A)$, and the quotient space $Y/\mathcal{R}(A)$ are finite-dimensional.*

The index of A is the integer defined by

$$ind(A) = \dim \mathcal{N}(A) - \dim(Y/\mathcal{R}(A)).$$

Let $F : \Omega \to \mathcal{L}(X, Y)$ be a holomorphic operator function on Ω. Denote by $\Phi_0(\Omega, \mathcal{L}(X, Y))$ the set of holomorphic Fredholm operator functions of index zero [13]. We assume that $F \in \Phi_0(\Omega, \mathcal{L}(X, Y))$, i.e., for each $\omega \in \Omega$, $F(\omega) \in \mathcal{L}(X, Y)$ is a Fredholm operator of index zero. The operator eigenvalue problem is to find $(\omega, u) \in \Omega \times X$, $u \neq 0$, such that

$$F(\omega)u = 0. \tag{A.1}$$

The resolvent set $\rho(F)$ and the spectrum $\sigma(F)$ of F with respect to Ω are respectively defined as

$$\rho(F) = \{\omega \in \Omega : F(\omega)^{-1} \in \mathcal{L}(Y,X)\} \quad \text{and} \quad \sigma(F) = \Omega \backslash \rho(F). \tag{A.2}$$

Furthermore, we assume that $\rho(F) \neq \emptyset$. Then the spectrum $\sigma(F)$ has no cluster points in Ω and every $\omega \in \sigma(F)$ is an eigenvalue [19].

The dimension of $\mathcal{N}(F(\omega))$, the null space of $F(\omega)$ for an eigenvalue ω, is called the geometric multiplicity.

Definition 3. *An ordered sequence of elements $x_0, x_1, \ldots, x_k$ in X is called a Jordan chain of F at an eigenvalue ω if*

$$F(\omega)x_j + \frac{1}{1!}F^{(1)}(\omega)x_{j-1} + \ldots + \frac{1}{j!}F^{(l)}(\omega)x_0 = 0, \quad j = 0, 1, \ldots, k,$$

where $F^{(j)}$ denotes the jth derivative.

The length of any Jordan chain for an eigenvalue is finite. Denote by $m(F, \omega, x_0)$ the maximal length of a Jordan chain formed by an eigenfunction x_0. The maximal length of Jordan chains for an eigenvalue ω is denoted by $\kappa(F, \omega)$. Elements of any Jordan chain are called generalized eigenfunctions of ω.

Definition 4. *The closed linear hull of all generalized eigenfunctions of an eigenvalue ω, denoted by $G(\omega)$, is called the generalized eigenspace.*

A basis $x_0^1, \ldots, x_0^J$ of the eigenspace $\mathcal{N}(F(\omega))$ is called canonical if

(i) $m(F, \omega, x_0^1) = \kappa(F, \omega)$,

(ii) x_0^j is an eigenfunction of the maximal possible order belonging to some direct complement M_j in $\mathcal{N}(F(\omega))$ to the linear hull $\operatorname{span}\{x_0^1, \ldots, x_0^{j-1}\}$, i.e.,

$$m(F, \omega, x_0^j) = \max_{x \in M_j} m(F, \omega, x) \quad \text{for } j = 2, \ldots, J.$$

The numbers $m_j(F, \omega) := m(F, \omega, x_0^j)$, $j = 2, \ldots, J$, are called the partial multiplicities of ω. The number

$$m(\omega) := \sum_{j=1}^{J} m_j(F, \omega)$$

is called the algebraic multiplicity of ω and coincides with the dimension of the generalized eigenspace $G(\omega)$.

To approximate the eigenvalues of F, consider operator functions

$$F_n \in \Phi_0(\Omega, \mathcal{L}(X_n, Y_n)), \quad n \in \mathbb{N},$$

such that the following properties hold [19, 3].

(b1) There exist Banach spaces X_n, Y_n, $n \in \mathbb{N}$, and linear bounded mappings $p_n \in \mathcal{L}(X, X_n)$, $q_n \in \mathcal{L}(Y, Y_n)$ such that

$$\lim_{n\to\infty} \|p_n v\|_{X_n} = \|v\|_X,\ v \in X, \quad \lim_{n\to\infty} \|q_n v\|_{Y_n} = \|v\|_Y,\ v \in Y.$$

(b2) The sequence $\{F_n(\cdot)\}_{n\in\mathbb{N}}$ satisfies

$$\|F_n(\omega)\| \leq \infty \quad \text{for all } \omega \in \Omega, n \in \mathbb{N}.$$

(b3) $\{F_n(\cdot)\}_{n\in\mathbb{N}}$ approximates $F(\omega)$ for every $\omega \in \Omega$, i.e.,

$$\lim_{n\to\infty} \|F_n(\omega)p_n x - q_n F(\omega)x\|_{Y_n} = 0 \quad \text{for all } x \in X.$$

(b4) For any subsequence $x_n \in X_n, n \in N' \subset \mathbb{N}$ with $\|x_n\|_{X_n}, n \in N'$ bounded and

$$\lim_{N'\ni n\to\infty} \|F_n(\omega)x_n - q_n y\|_{Y_n} = 0$$

for some $y \in Y$, there exists a subsequence $N'' \subset N'$ and a $x \in X$ such that

$$\lim_{N''\ni n\to\infty} \|x_n - p_n x\|_{X_n} = 0.$$

If the above conditions are satisfied, one has the following abstract approximation result (see Section 2 of [20] or Theorem 2.10 of [3]).

Theorem 2. *Assume that* (b1)-(b4) *hold. For any $\omega \in \sigma(F)$ there exists $n_0 \in \mathbb{N}$ and a sequence $\omega_n \in \sigma(F_n), n \geq n_0$, such that $\omega_n \to \omega$ as $n \to \infty$. For any sequence $\omega_n \in \sigma(F_n)$ with this convergence property, one has that*

$$|\omega_n - \omega| \leq C\varepsilon_n^{1/\kappa},$$

where

$$\varepsilon_n = \max_{|\eta-\omega|\leq\delta} \max_{v\in G(\omega)} \|F_n(\eta)p_n v - q_n F(\eta)v\|_{Y_n},$$

for sufficiently small $\delta > 0$. Here $G(\omega)$ is generalized eigenspace of corresponding eigenvalue ω and κ is the maximum rank of eigenvectors associated to ω.

References

[1] W. Axmann and P. Kuchment, *An efficient finite element method for computing spectra of Photonic and Acoustic band-gap materials I. Scalar Case.* J. Comput. Phys. 150 (1999), pp. 468–481.

[2] I. Babuška and J. Osborn, *Eigenvalue Problems, Handbook of Numerical Analysis, Vol. II, Finite Element Methods (Part 1)*, Edited by P.G. Ciarlet and J.L. Lions, Elsevier Science Publishers B.V. (North-Holland), 1991.

[3] W.J. Beyn, Y. Latushkin and J. Rottmann-Matthes, *Finding eigenvalues of holomorphic Fredholm operator pencils using boundary value problems and contour integrals*, Integr. Equat. Oper. Theo. 78 (2014), no. 2, pp. 155–211.

[4] D. Boffi, *Finite element approximation of eigenvalue problems*, Acta Numer. 19 (2010), pp. 1–120.

[5] D. Boffi, M. Conforti and L. Gastaldi, *Modified edge finite elements for photonic crystals,* Numer. Math. 105 (2006), pp. 249–266.

[6] D. Boffi, F. Brezzi and M. Fortin, *Mixed Finite Element Methods and Applications.* Berlin: Springer-Verlag (2013).

[7] S.C. Brenner, L.R. Scott, *The Mathematical Theory of Finite Element Methods*, 3rd ed. New York: Springer-Verlag (2008).

[8] C.T. Chan, Q.L. Yu and K.M. Ho, *Order-N spectral method for electromagnetic waves,* Phys. Rev. B 51 (1995), 16635.

[9] D.C. Dobson, *An efficient method for band structure calculations in 2D photonic crystals,* J. Comput. Phys. 149 (1999), pp. 363–376.

[10] D.C. Dobson, J. Gopalakrishnan and J.E. Pasciak, *An efficient method for band structure calculations in 3D photonic crystals,* J. Comput. Phys. 161 (2000), pp. 668–679.

[11] D.C. Dobson and J.E. Pasciak, *Analysis of an algorithm for computing electromagnetic Bloch models using Nedelec spaces,* Comput. Meth. Appl. Math. 1 (2001), pp. 138–153.

[12] B. Gong, J. Sun, T. Turner and C. Zheng, *Finite element/holomorphic operator function method for the transmission eigenvalue problem.* Math. Comput. 91 (2022), pp. 2517-2537.

[13] I. Gohberg and J. Leiterer, *Holomorphic Operator Functions of One Variable and Applications,* Birkhaluser Verlag, Basel, 2009.

[14] K.M. Ho, C.T. Chan, and C.M. Soukoulis, *Existence of a photonic gap in periodic dielectric structures,* Phys. Rev. Lett. 65 (1990), 3152.

[15] R. Huang, A. Struthers, J. Sun and R. Zhang, *Recursive integral method for transmission eigenvalues,* J. Comput. Phys. 327 (2016), pp. 830–840.

[16] R. Huang, J. Sun and C. Yang, *Recursive integral method with Cayley transformation,* Numer. Linear Algebra Appl. 25 (2018), no. 6, e2199.

[17] R. Huang, J. Sun and C. Yang, *A multilevel spectral indicator method for eigenvalues of large non-Hermitian matrices,* CSIAM Trans. Appl. Math. 1 (2020), no. 3, pp. 463–477.

[18] J.D. Joannopoulos, R.D. Meade and J.N. Winn, *Photonic Crystals: Molding the Flow of Light*, Princeton Univ. Press, Princeton, 1995.

[19] O. Karma, *Approximation in eigenvalue problems for holomorphic Fredholm operator functions. I,* Numer. Funct. Anal. Optim. 17 (1996), no. 3-4, pp. 365–387.

[20] O. Karma, *Approximation in eigenvalue problems for holomorphic Fredholm operator functions. II. (Convergence rate),* Numer. Funct. Anal. Optim. 17 (1996), no. 3-4, pp.389–408.

[21] F. Kikuchi, *Mixed and penalty formulations for finite element analysis of an eigenvalue problem in electromagnetism,* Comput. Methods Appl. Mech. Eng. 64 (1987), pp. 509–521.

[22] P. Kuchment, *Floquet Theory for Partial Differential Equations*, Birkhauser Verlag, Basel, 1993.

[23] C. Lackner, S. Meng and P. Monk, *Determination of electromagnetic Bloch variety in a medium with frequency-dependent coefficients,* J. Comput. Appl. Math. 358 (2019), pp. 359–373.

[24] D.S. Mackey, N. Mackey, C. Mehl and V. Mehrmann, *Vector spaces of linearizations for matrix polynomials,* SIAM J. Matrix Anal. Appl. 28 (2006), no. 4, pp. 971–1004.

[25] P. Monk, *Finite Element Methods for Maxwells Equations,* Oxford University Press, Oxford, 2003.

[26] J.B. Pendry and A. MacKinnon, *Calculation of photon dispersion relations,* Phys. Rev. Lett. 69 (1992), pp. 2772–2775.

[27] M. Qiu and S. He, *A nonorthogonal finite-difference time-domain method for computing the band structure of a two-dimensional photonic crystal with dielectric and metallic inclusions,* J. Appl. Phys. 87 (2000), pp. 8268–8275.

[28] A. Ruhe, *Algorithms for the nonlinear eigenvalue problem,* SIAM J. Numer. Anal. 10 (1973), 674-689.

[29] G.L. Sleijpen, G.L. Booten, D.R. Fokkema and H.A. van der Vorst, *Jacobi-Davidson type methods for generalized eigenproblems and polynomial eigenproblems,* BIT 36 (1996), no. 3, pp. 595–633.

[30] J. Sun and A. Zhou, *Finite Element Methods for Eigenvalue Problems,* CRC Press, Boca Raton, London, New York, 2016.

[31] O. Toader and S. John, *Photonic band gap enhancement in frequency-dependent dielectrics,* Phys. Rev. E 70 (2004), 046605.

[32] H. Voss, *An Arnoldi method for nonlinear eigenvalue problems,* BIT 44 (2004), pp. 387–401.

[33] W. Xiao, B. Gong, J. Sun and Z. Zhang, *A new finite element approach for the Dirichlet eigenvalue problem,* Appl. Math. Lett. 105 (2020), 106295.

[34] W. Xiao, B. Gong, J. Sun and Z. Zhang, *Finite Element Calculation of Photonic Band Structures for Frequency Dependent Materials,* J. Sci. Comput. 87 (2021), no. 1, pp. 1–16.